

## Destabilization of a Saffman-Taylor Fingerlike Pattern in a Granular Suspension

C. Chevalier,<sup>\*</sup> A. Lindner,<sup>†</sup> and E. Clément

Laboratoire de Physique et Mécanique des Milieux Hétérogènes (PMMH), UMR 7636 CNRS - ESPCI - Universités Paris 6 et 7,  
10, rue Vauquelin, 75231 Paris Cedex 05, France

(Received 23 May 2007; published 24 October 2007)

We study the Saffman-Taylor instability in a granular suspension formed by micrometric beads immersed in a viscous liquid. When using an effective viscosity for the flow of the suspension in the Hele-Shaw cell to define the control parameter of the system, the results for the finger width of stable fingers are found to be close to the classical results of Saffman-Taylor. One observes, however, an early destabilization of the fingers that can be attributed to the discrete nature of the individual grains. Classically, the threshold of destabilization is linked to the noise in the cell and is thus difficult to quantify. We show that the grains represent a “controlled noise” and produce an initial perturbation of the interface with an amplitude proportional to the grain size. The finite amplitude instability mechanism proposed by Bensimon *et al.* allows us to link this perturbation to the value of the threshold observed.

DOI: 10.1103/PhysRevLett.99.174501

PACS numbers: 47.15.gp, 47.54.-r, 47.55.Kf, 83.80.Hj

**Introduction.**—When a low viscosity fluid like air displaces a viscous fluid in a thin channel or Hele-Shaw cell, an instability develops at the interface, leading to the formation of fingerlike patterns. The viscous fingering or Saffman-Taylor instability [1] has received much attention not only because of its practical importance but also since it represents an archetype of many pattern forming systems [2–4]. Driven by practical and fundamental interests, several viscous fingering studies have lately been extended to non-Newtonian fluids where a wide variety of strikingly different patterns was found [5–7].

Here we study the Saffman-Taylor instability in a granular suspension, formed by micrometric polystyrene particles immersed in a silicon oil. Such suspensions are known to exhibit non-Newtonian properties such as, for example, normal stresses [8,9] or migration of particles toward zones of low shear rate [10,11]. Surprisingly we find that deviations from the classical finger width selection are small for a large number of experimental conditions when considering an effective viscosity for flow of the suspension in the confined geometry of the Hele-Shaw cell.

However, when increasing the finger velocity one observes an early destabilization of the fingers. For the classical Saffman-Taylor instability this has so far been attributed to the noise in the cell making it difficult to predict an exact threshold for this instability [12,13]. A mechanism for this destabilization was suggested theoretically [4] but has to our knowledge not been proven experimentally. We show that the individual particles immersed in the viscous liquid play the role of a controlled noise which allows us to study the mechanism of destabilization of the fingering patterns in detail and to link it to the theoretical predictions.

**Setup and characterization of the suspensions.**—The experiments are performed in an Hele-Shaw cell of length 1 m formed by two 1.5 cm thick glass plates separated by a thin mylar spacer (Fig. 1). The cell thickness  $b$  can be

varied ( $b = 0.75\text{--}1.43$  mm), as can the width  $W$  of the channel ( $W = 2\text{--}4$  cm). The thin channel is initially filled with a granular suspension that is then displaced by air. The suspensions are formed by spherical polystyrene beads from Dynoseeds with different grain diameters  $D = 20, 40, 80,$  or  $140$   $\mu\text{m}$  and density  $\rho = 1050\text{--}1060$   $\text{kg}/\text{m}^3$ . The grains are dispersed in a modified silicon oil (Shin Etsu SE KF-6011), such as to obtain density matching at a value  $\rho = 1070$   $\text{kg}/\text{m}^3$ . We measured the viscosity of the pure fluid  $\eta_0 = 191$   $\text{mPa}\cdot\text{s}$  as well as its surface tension  $\gamma = 21 \pm 1$   $\text{mN}/\text{m}$  at  $21$   $^\circ\text{C}$ . Note that the surface tension is not altered by the addition of grains. We have work with varying volume fractions, but remain below 40%, which allows us to avoid jamming problems and wall slip occurring at higher volume fractions.

A constant overpressure is applied at the inlet whereas the outlet is maintained at atmospheric pressure. The advancing fingertip is observed using a CCD camera mounted on a movable system which allows a manual tracking of its position. The camera is coupled to a micro-

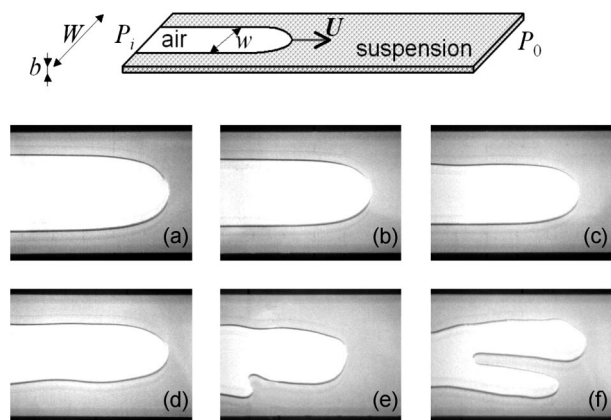


FIG. 1. Schematic drawing of the experimental setup. Evolution of a typical finger with increasing finger velocity (a)–(f).

computer for direct image acquisition. Note that in this configuration, the applied pressure gradient is not constant and, therefore, the finger accelerates when propagating through the cell. We have verified that this acceleration is slow enough and does not influence the observed finger properties (i.e., for a given tip velocity, we have no dependence on the applied overpressure).

*Stable fingers.*—For Newtonian fluids, the width  $w$  of the viscous fingers is determined by the capillary number  $\text{Ca} = \eta U / \gamma$ , which is the ratio of viscous to capillary forces,  $U$  being the finger velocity,  $\eta$  the viscosity, and  $\gamma$  the surface tension of the fluid. More precisely, the relative finger width  $\lambda = w/W$  is a function of the dimensionless control parameter  $1/B = 12(W/b)^2 \text{Ca}$ , which involves the cell aspect ratio. The mean flow (averaged over the cell thickness) is governed by Darcy's law which reduces far away from the finger to:  $V = -\frac{b^2}{12\eta} \nabla P$  with  $\nabla P$  being the applied pressure gradient and  $V$  the flow velocity.

We characterize the stable fingers and seek to establish the relevant control parameter for the system. A first step is to measure the suspension viscosity as a function of volume fraction. Flow in the confined geometry of the Hele-Shaw cell, where high gradients of shear rate are observed, might lead to flow inhomogeneities due to migration of particles towards zones of low shear rate [10]. We will thus compare the viscosity extracted directly from Darcy's law characterizing the flow in the Hele-Shaw cell to the one obtained from a commercial rheometer.

The suspension viscosities are obtained by rheological measurements using a double Couette geometry rheometer (Haake-RS600) of gap width  $2 \times 0.25$  mm and mean radius 20 mm. The gap width being small with respect to the radius, the local shear rate in the gap can be considered as uniform. In the range of shear rates tested ( $\dot{\gamma} = 0.1\text{--}100$  s $^{-1}$ ) corresponding also to the typical shear rates of the Hele-Shaw experiments, the suspensions behave as a Newtonian fluid with a viscosity  $\eta_{\text{Rh}}(\phi)$  well described by models used in recent literature (as, for example, Zarraga *et al.* [8]) [Fig. 2(a) open symbols]. These results confirm that particle migration is indeed negligible and indicate the

absence of particle aggregation in the range of volume fractions considered.

We investigate the rheology of our suspensions directly in the Hele-Shaw cell. To do so, we systematically establish a Darcy's law for all suspensions and cell geometries considered. The details of the procedure can be found in Refs. [14,15]. The results indicate the existence of an effective viscosity specific for flow in a Hele-Shaw cell  $\eta_C(\phi)$ . This viscosity was found to be independent of the cell geometry (i.e.,  $b$  and  $W$ ) as well as the grain diameter  $D$  and is only function of the volume fraction  $\phi$ .

We found for increasing  $\phi$  an increasing deviation of  $\eta_C$  from the corresponding rheometer viscosity  $\eta_{\text{Rh}}$  [Fig. 2(a) close symbols]. The fact that  $\eta_C$  is lower than  $\eta_{\text{Rh}}$  could be explained by the effect of particle migration to zones of low shear rate [10], here in the middle of the gap. In this case it has been observed that the flow profile deviates from an ideal parabolic profile and evolves towards a flatter profile [11], independent of  $V$  and solely dependent on  $\phi$ . This should lead to a lower flow resistance and thus to a lower effective viscosity. A steady profile is only reached after a certain flow distance [11] below which we do not consider our data.

We then systematically study the selection of the finger width for stable fingers for different values of the volume fraction  $\phi$ . Typical results are displayed on Fig. 2(b) and 2(c). The solid line represents the pure fluid measurements and thus corresponds to the classical result for Newtonian fluids. Importantly, we choose  $\eta_C(\phi)$  to define the control parameter  $1/B = 12(W/b)^2(\eta_C U / \gamma)$ . We notice that this choice rescales our data well when the ratio between the cell thickness and the grain diameter is larger than approximately 10. Below  $b/D \sim 10$  significant deviations from the classical result appear: fingers are slightly larger for low  $1/B$ , thinner for intermediate  $1/B$ —this narrowing is more important for large volume fraction—and then  $\lambda$  seems to join the classical curve for larger values of  $1/B$ .

The details of the selection mechanism of the viscous fingers can so far not be explained and are outside of the scope of this Letter. However, in all cases, for large  $1/B$  the

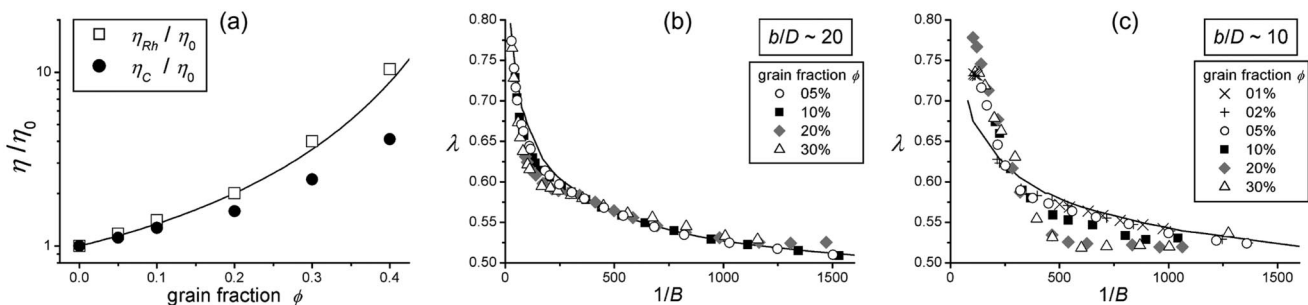


FIG. 2. (a) Relative viscosity of the suspensions ( $D = 80$   $\mu\text{m}$ ) as a function of the grain fraction  $\phi$  obtained from rheological measurements  $\eta_{\text{Rh}}(\phi)/\eta_0$  ( $\square$ ) and from flow in the Hele-Shaw cell  $\eta_C(\phi)/\eta_0$  ( $\bullet$ ). The solid line represents the prediction of Zarraga *et al.* [8]. (b) and (c) Relative finger width  $\lambda$  as a function of  $1/B = 12(W/b)^2(\eta_C U / \gamma)$  for the same suspensions. Cell width  $W = 4$  cm and cell thickness  $b = 1.43$  mm (b) and  $b = 0.75$  mm (c). The solid line represents the results for pure fluid.

classical results of Saffman and Taylor are recovered and the fingers can thus at this stage be considered as “normal” viscous fingers.

*Finger destabilization.*—When increasing the finger velocity and thus the control parameter  $1/B$  even further one observes a destabilization of these normal fingers. First, the sides of the fingers start to undulate and when the velocity is further increased, the finger becomes unstable by tip splitting. A typical evolution of such a destabilization can be seen in Fig. 1. Note that in some cases asymmetric fingers (not shown here) like those predicted by Ben Amar *et al.* [16] are observed.

This destabilization scenario is also observed in classical Saffman-Taylor experiments and has so far been attributed to the noise in the cell, hence making it difficult to predict exact values for this instability threshold [12,13]. In the case of our suspension, we measure the fluctuations  $\delta\lambda$  of the finger width by image processing [Fig. 3(a)] and detect the onset of growth of these fluctuations [Fig. 3(b)] defining the stability threshold and, therefore, the critical control parameter  $1/B_c$ .

When plotting the values of  $1/B_c$  against grain fraction (Fig. 4) for two different set ups (different cell thickness, same grain size), we surprisingly find that as soon as a small amount of grains (as small as 1%) is added, the value of the threshold drops strongly and thereafter is constant within the experimental uncertainties. We find different values for the threshold in pure fluid for the different configurations and thus two different intrinsic levels of noise. However, in the presence of grains the value of the threshold is well defined.

When looking closer at the destabilization scenario of a single finger (Fig. 4 inset), one observes that perturbations nucleate close to the fingertip and are then advected to the side of the finger. A possible explanation for this destabilization mechanism was given by Bensimon *et al.* [4]. They proposed that a perturbation nucleates at the fingertip, where the normal velocity is the highest and where the growth rate (given by the linear stability analysis of the Saffman-Taylor problem [17]) is the largest. While the finger continues to grow, the perturbation is advected to

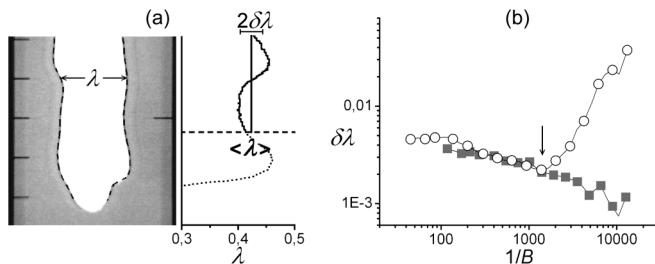


FIG. 3. (a) Image processing and measurement of the fluctuation of the relative finger width. (b)  $\delta\lambda$  as a function of  $1/B$  for pure fluid (■) and a suspension (○) ( $\phi = 10\%$ ,  $D = 80 \mu\text{m}$ ) in a cell geometry of  $W = 4 \text{ cm}$   $b = 1.43 \text{ mm}$ . The arrow indicates the stability threshold  $1/B_c$ .

the side of the finger where the normal velocity goes to zero and, thus, the perturbation growth stops. In the process of advection, the perturbation is stretched and, consequently, its amplitude is decreased. For a given control parameter  $1/B_c$ , one needs a given, finite amplitude of the initial perturbation  $A_i$  to be able to obtain a perturbation with a given final amplitude  $A_f$  when the side of the finger is reached. More quantitatively, Bensimon *et al.* derived the following relation that describes the “finite amplitude instability”:

$$A_f \approx A_i \exp(0.106 1/B_c^{1/2}). \quad (1)$$

In the following, we test if the destabilization observed in our situation can be described by this mechanism and if the existence of grains in the viscous fluid can be directly linked to the instability onset. A first indication is that we observe a destabilization threshold hardly affected by an increase of the grain fraction; the above described mechanism is indeed independent of the wavelength of the perturbation which one might be tempted to link to the grain fraction. In their theoretical approach, Bensimon *et al.* [4] considered the final amplitude  $A_f$  to be proportional to the channel width  $W$ . For our analysis, we directly use the value of the fluctuations of the finger width  $\delta\lambda$  observed at  $1/B_c$ . Those are of course via the finger width proportional to  $W$  and we consider a sinusoidal form of the fluctuations leading to  $A_f = \delta\lambda W 2\sqrt{2}$ . A natural assumption is to relate the amplitude of the initial perturbation  $A_i$  to the grain diameter  $D$ :  $A_i \propto D$ . We have performed experiments for different grain sizes  $D$  and different cell widths  $W$ . When we plot  $\sqrt{1/B_c}$  as a function of  $\ln(A_f/D)$  obtained for  $\phi = 10\%$ , different cell geometries, and different grain sizes (Fig. 5), we obtain a very satisfying quantitative agreement with the theoretical result of Bensimon *et al.*, when the only free parameter, the amplitude of the initial perturbation, is taken to be  $A_i \approx D/20$ . Unfortunately,

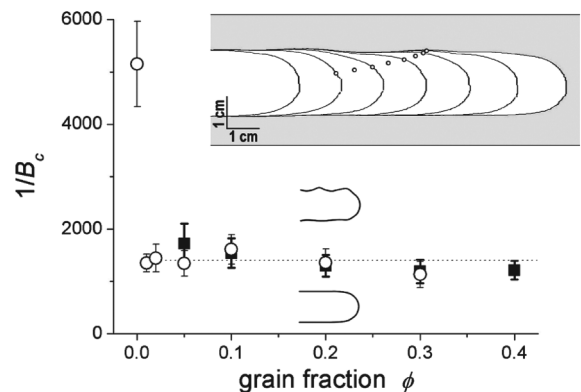


FIG. 4. Control parameter  $1/B_c$  at the stability threshold as a function of grain fraction  $\phi$ .  $D = 80 \mu\text{m}$ ,  $W = 4 \text{ cm}$ ,  $b = 0.75 \text{ mm}$  (○) and  $b = 1.45 \text{ mm}$  (■) (not shown here:  $1/B_c > 15000$  for pure fluid). Inset: Localization of the perturbation (○) during a typical experimental finger destabilization.

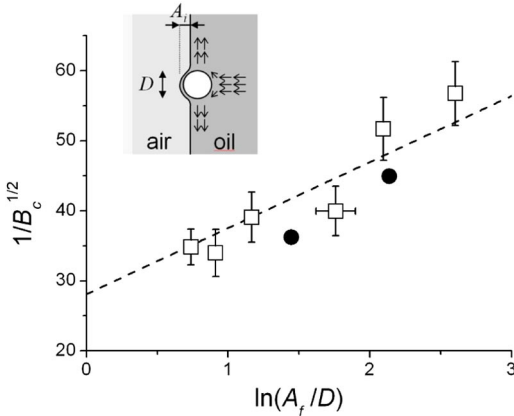


FIG. 5 (color online). Experimental values ( $\square$ ) and theoretical prediction from Bensimon *et al.* (solid line). Experiments performed by changing the grain diameter  $D = 20, 40, 80,$  and  $140 \mu\text{m}$ , the cell thickness  $b = 0.75\text{--}1.43 \text{ mm}$  and the cell width  $W = 2\text{--}4 \text{ cm}$ . Additional experiments ( $\bullet$ ) using a different silicon oil (Dow Corning 704). Inset: Schematic drawing of a particle approaching a free interface in a stagnation point flow.

experimental limitations on grain size and cell width do not allow us to extend the range of  $\ln(A_f/D)$  further with our setup.

Now, we need to show that a particle approaching a free interface at a stagnation point flow (Fig. 5 inset), as is the case of the fingertip, is indeed able to deform this interface with the correct amplitude. Hoffman [18] and Montiel *et al.* [19] established a link between the free interface amplitude of perturbation and a capillary number defined on the scale of a particle:  $\text{Ca}_p = \frac{2}{3} \frac{D}{b} \text{Ca}$ . In our case, the range of capillary numbers is  $\text{Ca}_p = 5 \times 10^{-3}\text{--}2 \times 10^{-2}$  and, thus, the corresponding values for the amplitude of the perturbation are of order of  $0.02\text{--}0.1 \times D$ . Therefore, this is indeed in good agreement with our result for the amplitude of the initial perturbation and it confirms the validity of the theoretical prediction of Bensimon *et al.* [4]. The grains of the suspension act here as a controllable noise amplitude.

**Conclusion.**—We have studied the destabilization of Saffman-Taylor fingers in a granular suspension. We have shown that the grains perturb the interface between the air and the suspension and lead to a premature destabilization of the fingers. This local perturbation is a function of the grain size and leads to lateral oscillations of the finger with a fixed amplitude at a certain instability threshold  $1/B_c$ . This threshold is found to be in good agreement with the theoretical predictions of Bensimon *et al.* given for this finite amplitude instability. To our knowledge this is the first time that an experiment allows to control the initial “noise” in the cell, typically considered to be re-

sponsible for the destabilization, allowing in this way to investigate directly this mechanism.

Recently a number of studies have reported oscillations of the finger width, observed, for example, for low capillary number [20] or fixed perturbations of the cell thickness [21]. A more close characterization of the oscillations resulting from the premature destabilization in our system might reveal similarities between the different systems.

We wish to thank Michel Cloître and Fabrice Monti for help with the rheological measurements, Daniel Bonn for help and advice with the experimental setup, and José Lanuza for technical assistance.

\*Present address: Laboratoire Central des Ponts et Chaussées, Paris, France

†lindner@ccr.jussieu.fr

- [1] P. Saffman and G. Taylor, Proc. R. Soc. A **245**, 312 (1958).
- [2] Y. Couder, *Growth Patterns: From Stable Curved Fronts to Fractal Structures* (Plenum Press, New York, 1991).
- [3] G. Homsy, Annu. Rev. Fluid Mech. **19**, 271 (1987).
- [4] D. Bensimon, L. Kadanoff, S. Liang, B. Shraiman, and C. Tang, Rev. Mod. Phys. **58**, 977 (1986).
- [5] K. McCloud and J. Maher, Phys. Rep. **260**, 139 (1995).
- [6] A. Lindner, D. Bonn, E. C. Poire, M. Ben Amar, and J. Meunier, J. Fluid Mech. **469**, 237 (2002).
- [7] H. Tang, W. Grivas, D. Homentcovschi, J. Geer, and T. Singler, Phys. Rev. Lett. **85**, 2112 (2000).
- [8] I. E. Zarraga, D. A. Hill, and D. Leighton, J. Rheol. (N.Y.) **44**, 185 (2000).
- [9] A. Singh and P. R. Nott, J. Fluid Mech. **490**, 293 (2003).
- [10] D. Leighton and A. Acrivos, J. Fluid Mech. **181**, 415 (1987).
- [11] M. Lyon and L. Leal, J. Fluid Mech. **363**, 25 (1998).
- [12] C. Park and G. Homsy, Phys. Fluids **28**, 1583 (1985).
- [13] P. Tabeling, G. Zocchi, and A. Libchaber, J. Fluid Mech. **177**, 67 (1987).
- [14] C. Chevalier, M. Ben Amar, D. Bonn, and A. Lindner, J. Fluid Mech. **552**, 83 (2006).
- [15] C. Chevalier, A. Lindner, and E. Clément, in *Powders and Grains*, edited by R. Garcia-Rojo, H. J. Herrmann and S. McNamara (A.A. Balkema, Rotterdam, 2005), pp. 1061–1065.
- [16] M. Ben Amar and E. Brener, Physica (Amsterdam) **D98**, 128 (1996).
- [17] R. Chuoke, P. v. Meurs, and C. v. d. Poel, Trans. Am. Inst. Min., Metall. Pet. Eng. **216**, 188 (1959).
- [18] R. L. Hoffman, J. Rheol. (N.Y.) **29**, 579 (1985).
- [19] R. Montiel and R. Alexander-Katz, J. Polym. Sci., B, Polym. Phys. **41**, 1362 (2003).
- [20] M. Moore, A. Juel, J. Burgess, W. McCormick, and H. Swinney, Phys. Rev. E **65**, 030601(R) (2002).
- [21] M. Torralba, J. Ortin, A. Hernandez-Machado, and E. C. Poire, Phys. Rev. E **73**, 046302 (2006).